Generating a nonperturbative mass gap using Feynman diagrams in an asymptotically free theory

Venkitesh Ayyar and Shailesh Chandrasekharan

Phys. Rev. D **96**, 114506 — Published 8 December 2017

DOI: 10.1103/PhysRevD.96.114506

Generating a non-perturbative mass gap using Feynman diagrams in an asymptotically free theory

Venkitesh Ayyar
Department of Physics, University of Colorado, Boulder, Colorado 80309, USA

Shailesh Chandrasekharan
Department of Physics, Box 90305, Duke University, Durham, North Carolina 27708, USA

Using the example of a two dimensional four-fermion lattice field theory we demonstrate that Feynman diagrams can generate a mass gap when massless fermions interact via a marginally relevant coupling. We introduce an infrared cutoff through the finite system size so that the perturbation series for the partition function and observables become convergent. We then use the Monte Carlo approach to sample sufficiently high orders of diagrams to expose the presence of a mass gap in the lattice model.

PACS numbers: 71.10.Fd,02.70.Ss,11.30.Rd,05.30.Rt

I. INTRODUCTION

Understanding how a mass gap is generated in an asymptotically free theory like Yang-Mills theory continues to be a fascinating topic of research. Using Wilson's lattice formulation the origin of the mass gap is easy to derive within the strong coupling expansion [1]. Monte Carlo calculations have shown that the mass gap continues to exist and scales appropriately even for much weaker couplings. However, the challenge is to begin with a weak coupling expansion and show the presence of the mass gap. A Monte Carlo method that directly works within the weak coupling expansion could perhaps shed more light on the subject.

Recently, Monte Carlo methods have emerged that sample weak coupling Feynman diagrams in a variety of models [2–7]. Can such methods also be applicable to asymptotically free theories like Yang Mills theories and QCD? The obvious problem is that the weak coupling approach is an expansion in powers of the coupling g, while mass gaps in these theories arise non-perturbatively through an essential singularity of the form $M \sim \mathrm{e}^{-\beta/g^2}$. So, at least naively, it seems impossible that weak coupling diagrams can be combined with Monte Carlo methods to generate a mass gap. As a first step in addressing this impasse, one can even ignore complications of a gauge theory and ask whether these weak coupling approaches can generate a mass gap in simpler two dimensional spin models that are known to be asymptotically free. This question was raised recently and partially addressed within the context of the two dimensional $O(N)$ and $U(N) \times U(N)$ model in the large N limit [8, 9]. The strategy that seems to work is to regulate the infrared divergences in a controllable way so as to make the weak coupling series convergent. A resummation of the convergent series then exposes the existence of the mass gap. Other non-perturbative approaches have also been used to compute mass gaps in two dimensional non-linear sigma models at large values of N [10–12].

Instead of two dimensional non-linear sigma models, in this work we consider an $SU(4)$ symmetric two dimensional four-fermion model. Such models are known to be asymptotically free [13, 14], and have a completely convergent weak coupling expansion when formulated on a finite space-time lattice. Thus, they are ideally suited to explore the question of whether Feynam diagrams can generate a non-perturbative mass gap. However, without the simplifications of large N, the weak coupling diagrammatic series may converge only after summing over many terms. In our model we accomplish this by using a Monte Carlo sampling procedure, since there are no sign problems. Thus, we are able to expose the presence of a non-perturbative mass gap that is independent of the infrared regulator. By tuning the bare coupling to zero we can also explore the continuum limit. From a continuum quantum field theory perspective, we believe there are connections of our approach to recent ideas of using resurgent functions and trans-series combined with boundary conditions that control infrared divergences to define the perturbation series non-perturbatively [15–17].

The physics of our $SU(4)$ symmetric lattice model is interesting from other perspectives as well. For example it was recently studied extensively in three and four dimensions [18–22] and contains a weak coupling massless fermion phase and a strong coupling massive fermion phase without any spontaneous symmetry breaking. In three dimensions one finds a second order phase transition that separates these two phases. This quantum critical point is exotic and may contain emergent gauge fields [23]. We believe this critical point moves to the origin in two dimensions. Thus, the mass generation mechanism in our model is similar to the one discussed in [24].

II. LATTICE MODEL

Two dimensional lattice four-fermion models have been studied extensively using Monte Carlo methods in the past, but mostly within the Wilson fermion formulation [25–29]. Efficient Monte Carlo methods have also been designed using the worldline representation [30, 31]. However, none of these studies have focused on the question whether weak coupling perturbation theory using Feynman diagrams can generate a non-perturbative mass gap. A simple model that is suitable for addressing this question is the reduced staggered fermion model whose action is given by

$$S(\psi) \;=\; \frac{1}{2}\sum_{x,y,a}\; \psi^a_x\, M_{x,y}\, \psi^a_y \;-\; U\,\sum_x\; \psi^4_x\psi^3_x\psi^2_x\psi^1_x, \quad (1)$$

where $M_{x,y}$ is the free staggered fermion matrix

$$M_{x,y} \;=\; \frac{1}{2}\sum_{\alpha}\,\eta_{\alpha,x}\,\big(\delta_{x+\hat{\alpha},y}-\delta_{x-\hat{\alpha},y}\big), \qquad (2)$$

with the phase factors $\eta_{1,x}=1$, $\eta_{2,x}=(-1)^{x_1}$ and a labels the four flavors. We can obtain (1) by naively discretizing the continuum two dimensional model,

$$S_{\rm cont}=\int d^2x\,\Big\{\sum_{a,i,\alpha}\overline{\psi}^i_a(x)(\sigma_\alpha)_{ij}\partial_\alpha\psi^j_a(x) - U\Big(\psi^2_1(x)\psi^1_1(x)\psi^2_2(x)\psi^1_2(x)+\overline{\psi}^2_1(x)\overline{\psi}^1_1(x)\overline{\psi}^2_2(x)\overline{\psi}^1_2(x)\Big)\Big\}, \qquad (3)$$

on a space-time lattice and using the well known spin diagonalization transformation to reduce the fermion doubling [32, 33]. In the continuum model (3), the flavor index $a=1,2$ runs only over two values and $i=1,2$ refers to the spin. The matrices $\sigma_\alpha, \alpha=1,2$ are two Pauli matrices. Such a connection between the continuum model and a similar lattice model in four dimensions was recently discussed in [21, 34].

Note that there are no $\overline{\psi}^a_x$ fields in our lattice action. In the reduced staggered formulation, one keeps only the minimimal number of fermion fields per site and defines them as ψ^a_x on all sites. The partition function of our model is given by

$$Z=Z_0\int[d\psi]\;{\rm e}^{-S(\psi)} \qquad (4)$$

where Z_0 is a constant chosen so that $Z=1$ in the free theory. The Grassmann integration measure $[d\psi]$ is a product of $(d\psi^1_x d\psi^2_x d\psi^3_x d\psi^4_x)$ on every site x.

At $U=0$, when we focus on the physics at very large length scales as compared to the lattice spacing, our model will describe four flavors of free massless (two-component) Dirac fermions. As a probe of the long distance physics we can take space-time to be a torus of side L (in lattice units) in each direction with anti-periodic boundary conditions. In two dimensions, a free fermion field is expected to have a mass dimension $[\psi^i_a]=1/2$, which means the fermion propagator has the mass dimension of one and must decay as $G_f(x,y)\sim 1/|x-y|$ for large separations. In Fig. 1 we plot the scaling of the propagator at a separation of $|x-y|=L/2$ along one of the directions, $R=G_f(0,L/2)$ as a function of L and find that $R\sim 1.671/L$. In the same figure we also show the scaling of the susceptibility

$$\chi_1=\frac{1}{2Z}\int[d\psi]{\rm e}^{-S}\;\sum_y\Big\{\psi^a_0\psi^b_0\psi^b_y\psi^a_y\Big\}, \qquad (5)$$

as a function of L. From continuum power counting, χ_1 is expected to be dimensionless and can only have a logarithmic dependence on L. Indeed we see that it diverges logarithmically. We will see later that U, which is also expected to be dimensionless perturbatively, becomes marginally relevant and generates an exponentially small mass gap when $U>0$. This is consistent with asymptotic freedom as predicted originally by Gross and Neveu [13].

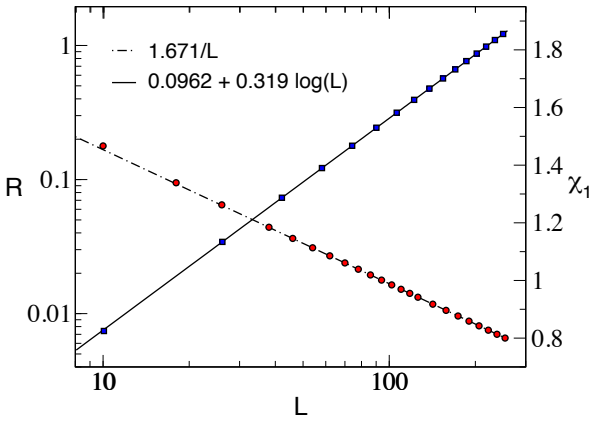

FIG. 1: Scaling of the fermion propagator at the mid point (R) and the susceptibility (χ_1) as a function of L in the free theory.

III. THE PARTITION FUNCTION

When the partition function of our model is expanded in powers of the coupling U,

$$Z \;=\; \sum_k z_k U^k \;=\; \sum_k\Big(\sum_{[x;k]}\Omega([x;k])\Big)\,U^k, \qquad (6)$$

the coefficients z_k can be written as a sum over weights of all possible vertex configurations $[x;k]=\{x_1,x_2,...,x_k\}$. Each vertex configuration is an ordered set of k different lattice sites where interactions occur and its weight

$$\Omega([x;k]) \;=\; Z_0\prod_a\Big(\int[d\psi^a]{\rm e}^{-\frac{1}{2}\psi^a_x M_{x,y}\psi^a_y}\;\psi^a_{x_1}\psi^a_{x_2}...\psi^a_{x_k}\Big), \qquad (7)$$

can be computed as a sum over Feynman diagrams. For each flavor a the sum is given by the Pfaffian of a $k\times k$ matrix $W([x;k])$, whose matrix elements are given by the free staggered fermion propagator $G_f(x_i,x_j)$ between the sites in the vertex configuration [21]. Thus, we obtain

$$\Omega([x;k]) \;=\; \Big({\rm Pf}(W([x;k])\Big)^4, \qquad (8)$$

which is guaranteed to be positive. Hence we can use a Monte Carlo method to sample vertex configurations $[x;k]$ distributed according to the probability distribution

$$P_k(U,[x;k]) \;=\; \frac{U^k}{Z(U)}\Omega([x;k]). \qquad (9)$$

Due to symmetries of our model, only configurations $[x;k]$ with an equal number of even and odd sites have non-zero weights. This implies that only even values of k contribute to the expansion (6).

The partition function Z of four-fermion models like the one we study in our work, is a completely convergent series in U on a finite lattice. In our model since the maximum number of vertices that are allowed in the partition function is L^2, it

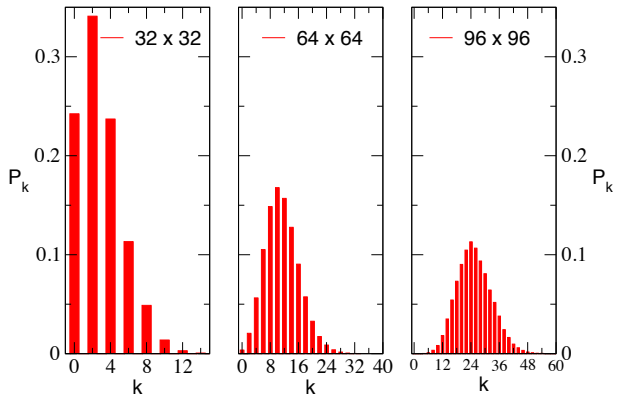

FIG. 2: Probability distribution of vertices in the partition function as a function of the lattice size at $U = 0.1$ for $L = 32, 64$ and 96. The average density of vertices $\rho_k = \langle k \rangle / L^2 \approx 0.00267$ remains constant in all the three cases.

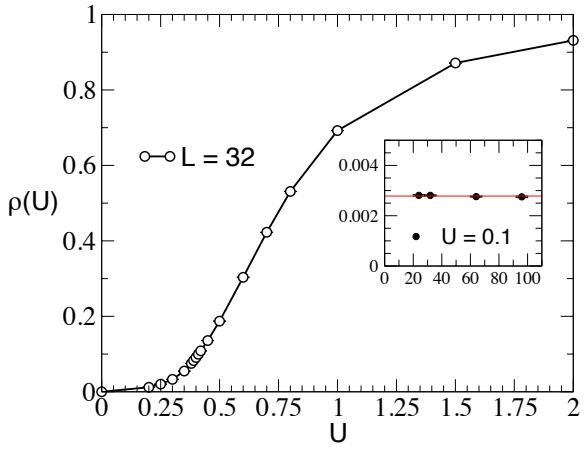

FIG. 3: Plot of the density of vertices $\rho(U)$ as a function of U. The inset shows the density at $U = 0.1$ as a function of L. We see that the density of vertices remains the same as L increases.

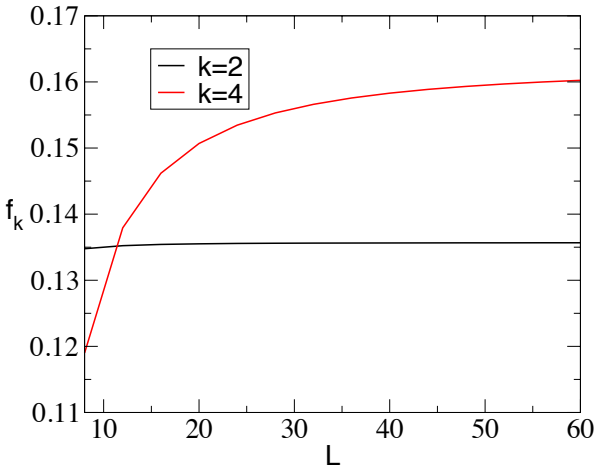

FIG. 4: Plot of the perturbative coefficients f_2 and f_4 in the expansion of the free energy as a function of L.

is in fact a polynomial. Thus, we wish to understand how the infrared divergences present in an asymptotically free theory arise from this polynomial as L^2 becomes large. In order to gain some insight into the dominant terms in the expansion we define the probability distribution $P_k(U) = z_k U^k / Z(U)$, which is the sum of $P_k(U, [x, k])$ over all vertex configurations $[x; k]$ with a fixed k. In Fig. 2 we plot this probability distribution of vertices at $U = 0.1$ for different values of L obtained using Monte Carlo sampling. As we can see, sectors with large number of vertices are suppressed exponentially and the average number of vertices is much smaller than the maximum value $k_{\max} = L^2$. We also discover that a more useful quantity is the average density of vertices $\rho(U) = \langle k \rangle / L^2$. In the inset of Fig. 3 we plot the density at $U = 0.1$ for various lattice sizes and observe that it does not change much as a function of L. At $U = 0.1$, the average density is $\rho = 0.0027$, but this changes with U as shown in the main plot.

It is easy to understand why the average density of vertices approaches a constant in the thermodynamic limit. From a statistical mechanics point of view one expects that the partition function scales as $Z = \exp(f(U)L^2)$ in the thermodynamic limit, where $f(U)$ is the free energy density. The average density of vertices is related to $f(U)$ through the relation

$$\rho(U) = \frac{\langle k \rangle}{L^2} = (U/L^2)(\partial \ln Z(U)/\partial U) = U(\partial f(U)/\partial U). \tag{10}$$

Since $f(U)$ is independent of the volume for sufficiently large volumes, so is $\rho(U)$. The connection between $Z(U)$ and $f(U)$ is well known in diagrammatic perturbation theory; the former contains contributions from disconnected diagrams, while the latter gets contributions only from connected diagrams. At a fixed value of L, like $Z(U)$ we can also expand $f(U) = f_2 U^2 + f_4 U^4 + ...$ and find connections between f_k's and z_k's. For example $f_2 = z_2/L^2$ and $f_4 = (z_4 - z_2^2/2)/L^2$ and so on.

From the discussion above, we know that $Z(U)$ is a polynomial in U on a finite lattice, but this is not the case for $f(U)$. In fact we cannot rule out the possibility that $f(U)$ will be divergent for some value of U even on a finite lattice. If there are infrared divergences in perturbation theory they would appear in f_k in the thermodynamic limit. In Fig. 4 we plot f_2 and f_4 as functions of L for our model and see that both these coefficients are well behaved and do not show infrared divergences. This seems to be a feature of our current model due to its symmetries. We have not explored higher order terms in this work. Note that even if the f_k's contained divergences, we can still extract $f(U)$ through the integral

$$f(U) = \int_0^U \rho(U)/U, \tag{11}$$

if we can compute $\rho(U)$ non-perturbatively by summing over

the distribution of vertices. In our work this is performed using the Monte Carlo method. Thus, the usual infrared divergences in perturbation theory disappear once this resummation is performed at every finite value of L.

IV. THE MASS GAP

In order to see how Feynman diagrams generate the mass gap in our model, we have studied two observables that are sensitive to the mass gap and both of them give very similar results [35]. Here we focus on one of them, which is the finite size susceptibility χ_1 defined in (5). As we already pointed out earlier, in the free theory χ_1 diverges logarithmically for large values of the lattice size L (see Fig. 1). However, if a mass gap M is generated in the fermion bilinear channel, we expect χ_1 to level off roughly around $L \sim M^{-1}$. The calculation of χ_1 can also be expressed as a sum over Feynman diagrams through the relation,

$$\chi_1 \;=\; \sum_{y,k} \Big(\sum_{[x;k]} \Gamma_{0,y}([x;k])\; P_k(U,[x;k]) \Big) \qquad (12)$$

where $\Gamma_{0,y}([x;k])$ is the ratio of two quantities. The numerator is the sum over all Feynman diagrams with two external sources $\psi_0^a \psi_0^b$ and $\psi_y^b \psi_y^a$, the former located at the origin and the latter at y, in addition to the configuration of interaction vertices $[x;k] = \{x_1, x_2, ..., x_k\}$. The denominator is $\Omega([x;k])$, i.e., the sum over Feynman diagrams without the sources. This ratio makes $\Gamma_{0,y}([x;k])$ scale like a "connected" Feynman diagram for large volumes since a factor that scales exponentially in the volume is cancelled between the numerator and the denominator.

In order to compute χ_1 we first generate vertex configurations $[x;k]$ with probability $P_k(U,[x;k])$. For each configuration we then compute $\Gamma_{0,y}([x;k])$ by choosing two source points, one chosen at random (which becomes the origin) and the other at the site y. We then sum over $\Gamma_{0,y}([x;k])$ obtained by varying y over all possible locations, while keeping the other source fixed. The value we thus obtain is a Monte Carlo estimate of χ_1 for the particular vertex configuration generated. If χ_1 contains infrared divergences, the Monte Carlo average of our estimates will increase indefinitely with L. At $U = 0$ the configurations $[x;k]$ generated are always trivial with no vertices (i.e., $k = 0$), and the value of χ_1 does increase with L as shown in Fig. 1. On the other hand, as we discussed above, in our model we expect χ_1 to level off when $L > M^{-1}$. In the left plot of Fig. 5 we show χ_1 as a function of L at $U = 0.3$ and 0.4. We observe that indeed χ_1 begins to level off around $L \sim 128$ at $U = 0.3$ and around $L \sim 32$ at $U = 0.4$. The fact that it takes substantially larger lattice sizes to level off at $U = 0.3$ as compared to $U = 0.4$ is an indication that M is decreasing rapidly. In the figure we also plot the $U = 0$ results for comparison.

Statistically speaking this implies that for most vertex configurations $[x;k]$ the Monte Carlo estimate of $\Gamma_{0,y}[x;k]$ begins to decay exponentially for points y far from the origin. This implies that the infrared divergences of perturbation theory disappear for sufficiently large lattices when we take into account a constant density of vertices. In other words we will need to consider large orders of perturbation theory, especially when U is small, before a mass gap will be observed. But what about divergences that we know exist at even small orders of perturbation theory? We believe these are the ones that cause the enhancement in χ_1 at small values of L (see left figure of Fig. 5) but eventually become statistically insignificant at large values of L. In other words they are rare and hidden in the Monte Carlo estimate of χ_1. We do see such rare fluctuations in our data. For example in Fig. 6 we plot the fluctuations in χ_1 during a sample of the Monte Carlo time history for $L = 64$ and $U = 0.4$. For these parameters a mass gap has been generated and χ_1 has almost saturated to

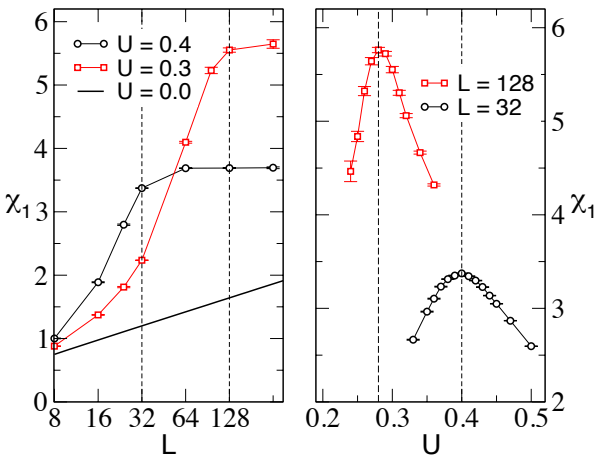

FIG. 5: Plot of the susceptibility χ_1 as a function of U for different lattice sizes. For value of L, we can define the mass scale $M_b' = 1/L$ that is generated when the location of the peak $U = U_{\rm p}$ determines the scale $M_b' = 1/L$.

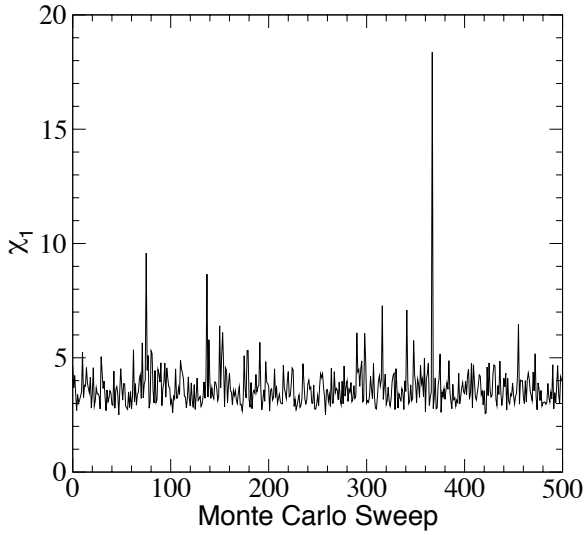

FIG. 6: Fluctuations of χ_1 in a sample of 500 vertex configurations generated consecutively during Monte Carlo sampling.

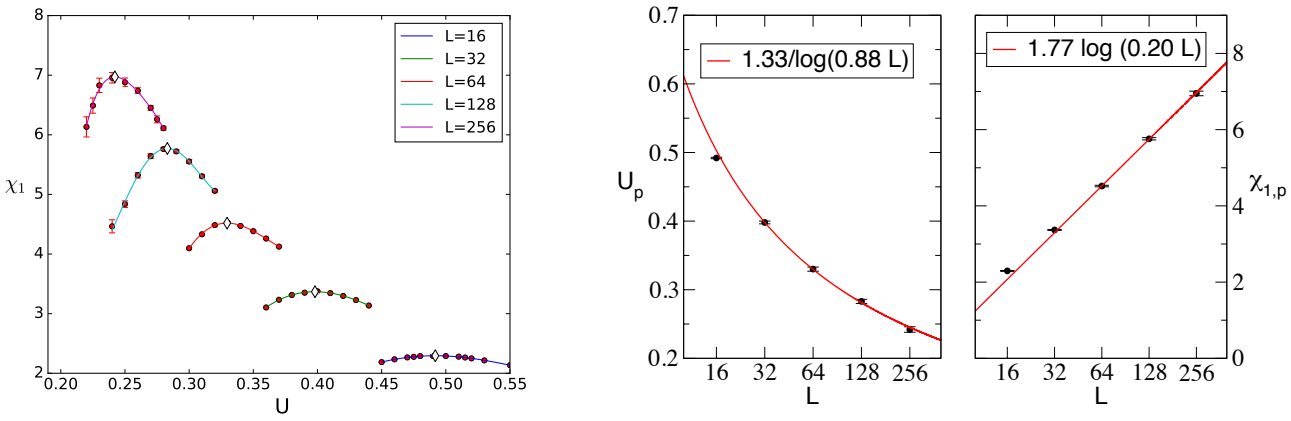

FIG. 7: (Left Figure) Plot of χ_1 as a function of U for different values of L. The locations of the peak are obtained by fitting the data to a quartic curve are listed in Tab. I. (Right Figure) Plot of $U_{\rm p}$ and $\chi_{1,\rm p}$ as a function of L and the fits to Eq.(13).

its thermodynamic value of approximately 3.7. However, as Fig. 6 shows there are still large but rare fluctuations in χ_1 that are five times larger than the average value. The fact that these divergent contributions will be rare as compared to finite contributions once the theory is regularized in the infrared, cannot be easily uncovered in usual perturbation theory.

For a quantitative analysis, instead of measuring the conventional mass gap M, in this work we define a slightly different mass scale M_b as follows. We first note that the susceptibility χ_1 has a peak when it is plotted as a function of U for a fixed value of L. This behavior is clearly visible in the right plot in Fig. 5, where χ_1 is plotted as a function of U at $L = 32$ and 128. For a fixed L if the peak in χ_1 occurs at $U = U_p$, then we define $M_b \equiv L^1$ as the non-perturbative mass scale generated at the coupling $U = U_p$. Comparing the left and right plots of Fig. 5 we see that our definition of M_b is also roughly consistent with the value of M obtained using the value of L where χ_1 begins to saturate. We have accurately located the peaks at various lattice sizes by fitting the data to quartic functions as shown in Fig. 7. Table I gives the values of these peaks along with systematic errors that arise from our fitting procedures [35].

L	$\chi_{1,\rm p}$	$U_{\rm p}$	L	$\chi_{1,\rm p}$	$U_{\rm p}$
16	2.293(2)	0.492(1)	32	3.368(5)	0.398(2)
64	4.520(20)	0.330(3)	128	5.760(30)	0.283(3)
256	6.950(60)	0.242(4)			

TABLE I: Fit values for $\chi_{1,\rm p}$ and $U_{\rm p}$ as a function of L.

In an asymptotically free theory we expect $M_b \sim \Lambda \exp(-\beta/U_{\rm p})$ at leading order. Further, since $\chi_{1,\rm p}$ is dimensionless it is expected to grow logarithmically in the continuum limit. Thus, for sufficiently large values of L we try to fit our data to the form

$$\chi_{1,\rm p} = \alpha \log(\Lambda_1 L), \quad U_{\rm p} = \frac{\beta}{\log(\Lambda_2 L)}. \qquad (13)$$

In Fig. 7 we show our results, which are consistent with both these expectations. The parameters obtained from the fit to our data are $\alpha = 1.77(4), \beta = 1.33(4)$, $\Lambda_1 = 0.20(1)$ and $\Lambda_2 = 0.88(9)$ [35]. It is usually difficult to match β with the results of one loop perturbation theory, since this can require extremely large correlation lengths [36]. On the other hand qualitative exponential scaling of mass gaps, as we do in the current work, can be observed more easily with lattice sizes like the ones we study in this work [37].

V. CONCLUSIONS

In this work we have shown how weak coupling Feynman diagrams can contain the information of a non-perturbative mass gap in an asymptotically free theory. Using a specific lattice model we first tamed the infrared divergences in the usual perturbation theory by formulating the problem in a finite volume. We then showed that the physics of the mass gap arises at sufficiently large volumes when we sample Feynman diagrams containing a finite density of interactions. The infrared divergences of the original perturbative expansion seem to be hidden in a few statistically insignificant vertex configurations. Our work suggests that a perturbative expansion organized in terms of Feynman diagrams containing a fixed density of interactions may be worth exploring. Exploring extensions of our work to gauge theories would also be interesting.

Acknowledgments

We thank T. Bhattacharya, S. Hands, R. Narayanan, U.-J. Wiese and U. Wolff for helpful discussions. The material presented here is based upon work supported by the U.S. Department of Energy, Office of Science, Nuclear Physics program under Award Number DE-FG02-05ER41368.

[1] J. B. Kogut, Rev. Mod. Phys. **51**, 659 (1979).
[2] N. V. Prokof'ev and B. V. Svistunov, Phys. Rev. Lett. **81**, 2514 (1998).
[3] N. Prokof'ev and B. Svistunov, Phys. Rev. Lett. **99**, 250201 (2007).
[4] M. Boninsegni, N. V. Prokof'ev, and B. V. Svistunov, Phys. Rev. E **74**, 036701 (2006).
[5] N. V. Prokof'ev and B. V. Svistunov, Phys. Rev. B **77**, 125101 (2008).
[6] E. Kozik, K. Van Houcke, E. Gull, L. Pollet, N. Prokofev, B. Svistunov, and M. Troyer, Europhys. Lett. **90**, 10004 (2010).
[7] G. Cohen, E. Gull, D. R. Reichman, and A. J. Millis, Phys. Rev. Lett. **115**, 266802 (2015).
[8] P. V. Buividovich, PoS **LATTICE2015**, 293 (2016), 1510.06568.
[9] P. V. Buividovich and A. Davody (2017), 1705.03368.
[10] C. Kopper, J. Magnen, and V. Rivasseau, Commun. Math. Phys. **169**, 121 (1995).
[11] C. Kopper, Commun. Math. Phys. **202**, 89 (1999).
[12] P. Orland, Phys. Rev. **D90**, 125038 (2014), 1410.2627.
[13] D. J. Gross and A. Neveu, Phys. Rev. D **10**, 3235 (1974).
[14] E. Witten, Nuclear Physics B **145**, 110 (1978), ISSN 0550-3213.
[15] G. V. Dunne and M. Unsal, JHEP **11**, 170 (2012), 1210.2423.
[16] G. V. Dunne and M. Unsal, Phys. Rev. **D89**, 041701 (2014), 1306.4405.
[17] A. Cherman, D. Dorigoni, G. V. Dunne, and M. Unsal, Phys. Rev. Lett. **112**, 021601 (2014), 1308.0127.
[18] V. Ayyar and S. Chandrasekharan, Phys. Rev. D **93**, 081701 (2016).
[19] V. Ayyar and S. Chandrasekharan, Phys. Rev. D **91**, 065035 (2015).
[20] S. Catterall, Journal of High Energy Physics **2016**, 121 (2016).
[21] V. Ayyar and S. Chandrasekharan, Journal of High Energy Physics **2016**, 58 (2016), ISSN 1029-8479.
[22] S. Catterall and D. Schaich, Phys. Rev. D **96**, 034506 (2017).
[23] Y.-Z. You, Y.-C. He, C. Xu, and A. Vishwanath (2017), 1705.09313.
[24] Y. BenTov, JHEP **07**, 034 (2015), 1412.0154.
[25] K.-I. Nagai and K. Jansen, Physics Letters B **633**, 325 (2006), ISSN 0370-2693.
[26] C. Gattringer, V. Hermann, and M. Limmer, Phys. Rev. D **76**, 014503 (2007).
[27] W. Bietenholz, E. Focht, and U. J. Wiese, Nucl. Phys. **B436**, 385 (1995).
[28] I. Ichinose and K. Nagao, Mod. Phys. Lett. **A15**, 857 (2000).
[29] S. Aoki and K. Higashijima, Prog. Theor. Phys. **76**, 521 (1986).
[30] O. Bar, W. Rath, and U. Wolff, Nucl. Phys. **B822**, 408 (2009), 0905.4417.
[31] T. Korzec and U. Wolff, PoS **LAT2006**, 218 (2006), hep-lat/0609022.
[32] H. Sharatchandra, H. Thun, and P. Weisz, Nucl.Phys. **B192**, 205 (1981).
[33] C. van den Doel and J. Smit, Nucl.Phys. **B228**, 122 (1983).
[34] S. Catterall and N. Butt (2017), 1708.06715.
[35] For further details about our work and analysis we refer the reader to the attached supplementary material.
[36] B. B. Beard, R. J. Birgeneau, M. Greven, and U.-J. Wiese, Phys. Rev. Lett. **80**, 1742 (1998).
[37] M. Creutz, Phys. Rev. Lett. **45**, 313 (1980).